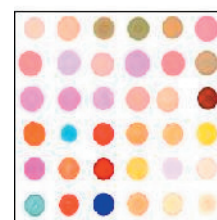


243

A perspective on four new porphyrin-based functional materials and devices

Charles Michael Drain*, Joseph T. Hupp, Kenneth S. Suslick, Michael R. Wasielewski, Xin Chen

A perspective on the formation and use of porphyrins as materials and as components of devices is given. Self-assembled, self-organized, and covalent porphyrin arrays for applications as sensors, sieves, catalysts and photonic devices are discussed as is arrays of metalloporphyrins and other dyes as cross-reactive sensors.

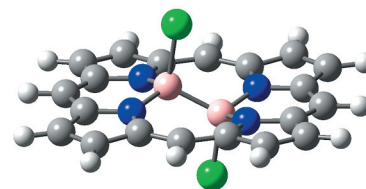


259

Recent developments in the coordination chemistry of porphyrin complexes containing non-metallic and semi-metallic elements

Penelope J. Brothers*

Recent advances in the chemistry of main group porphyrin complexes are surveyed, including boron and tellurium porphyrins which reveal unprecedented structural types, advances in the preparation and reactivity of Group 14 (silicon and tin) and Group 15 porphyrin complexes, and a discussion of out-of-plane distortions (ruffling) of light element Group 14 and 15 porphyrin complexes.

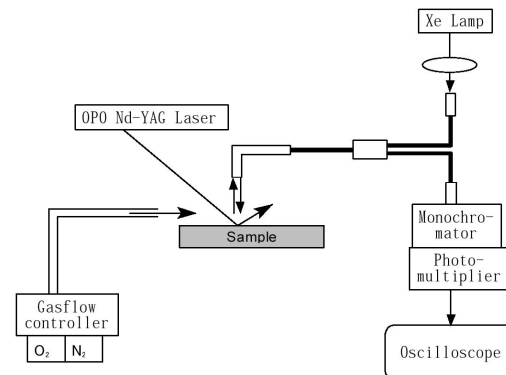


268

Overview of optical sensors using porphyrins

Ichiro Okura*

The background and the concept of optical sensor technology are briefly introduced and a new optical sensing system by triplet-triplet absorption is discussed as an example.

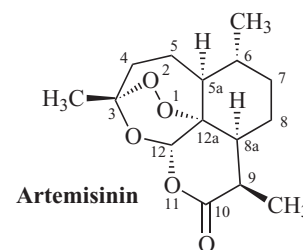


271

From studies on artemisinin derivatives to trioxaquinones

Bernard Meunier*

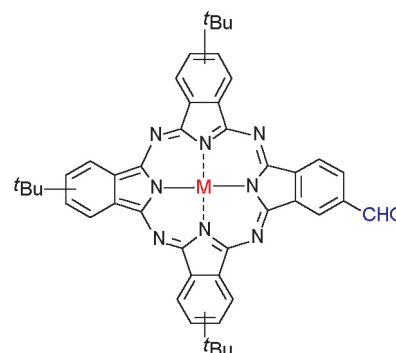
Artemisinin, an antimalarial trioxane is able to alkylate the heme after activation by heme itself via an electron transfer from the iron(II) to the endoperoxide function of the drug. Based on these mechanistic studies, new antimalarial agents (trioxaquinones) have been synthesized.



274
Synthetic advances in phthalocyanine chemistry

Gema de la Torre and Tomás Torres*

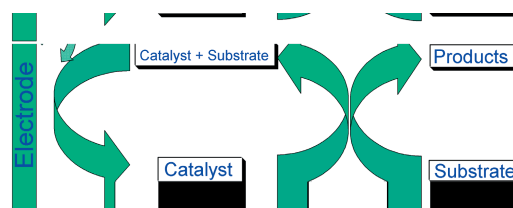
This overview is devoted to present the state-of-the-art in the preparation of low-symmetry phthalocyanine derivatives and analogues. New synthetic trends focused on the preparation of phthalocyanines and Pc analogues bound to other electronically active molecules are also treated.



285
Recent advances in the electrochemistry of porphyrins and phthalocyanines

Francis D'Souza*

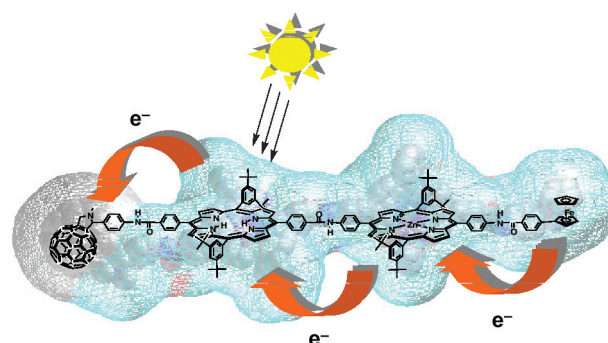
An overview of the recent developments in the electrochemistry of metalloporphyrins and metallophthalocyanines is presented by focusing briefly on the electroanalytical, electrocatalytic and electrochemical sensor applications.



289
Electron transfer in electron donor-acceptor ensembles containing porphyrins and metalloporphyrins

Dirk M. Guldi* and Shunichi Fukuzumi

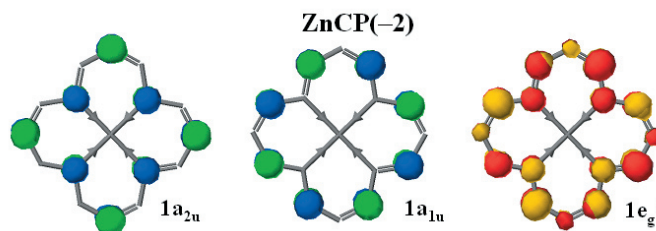
The function of porphyrins and metalloporphyrins in novel, redox- and lightactive donor-acceptor ensembles is critically reviewed. Besides acting as light harvesting antenna moieties, porphyrins and metalloporphyrins show particular benefits when used as electron donor components.



296
Theoretical aspects of the spectroscopy of porphyrins and phthalocyanines

Martin Stillman*, John Mack, and Nagao Kobayashi*

The development of theoretical models that describe the electronic structures of the porphyrins and phthalocyanines using ZINDO and DFT techniques is rapidly approaching the point where the major spectral bands over a wide energy range, for both symmetric and non-symmetric molecules can be fully accounted for.



301
Resonance Raman spectroscopy

Teizo Kitagawa*

A brief overview of topics and papers given in Kyoto at the ICPP-2 microsymposium on resonance Raman spectroscopy is presented.

A Perspective on Four New Porphyrin-Based Functional Materials and Devices

Charles Michael Drain,^{*a} Joeseeph T. Hupp^b, Kenneth S. Suslick,^c Michael R. Wasielewski,^b Xin Chen^a

^a*Department of Chemistry & Biochemistry, Hunter College of the City University of New York, 695 Park Avenue, New York, NY 10021*

^b*Department of Chemistry, Northwestern University, 2145 Sheridan Road, Evanston, IL 60208*

^c*Department of Chemistry, University of Illinois, 600 S. Mathews Avenue, Urbana-Champaign, IL 61801*

Received date (to be automatically inserted after your manuscript is submitted)

Accepted date (to be automatically inserted after your manuscript is accepted)

ABSTRACT: The tremendous potential for the manifold applications of porphyrins, porphyrazines, and phthalocyanines derives from their photophysical and electrochemical properties, their remarkable stability, and their predictable and rigid structure. These applications include nonlinear optics, catalysts, sensors, actuators, molecular sieves, and therapeutics. All of these properties are modulated by appending various chemical moieties onto the macrocycles, by choice of metallo derivative, and by the choice of environment. In multichromophoric systems, furthermore, the relative orientation of the chromophores, the nature of the linker, and the size of the system also dictate the properties. The synthesis of multichromophoric systems – both via covalent and noncovalent linkers – is driven by the desire to make new materials and to understand biological processes such as the various aspects of photosynthesis. Though electron and energy transfer processes continue to drive the synthesis of ever more complex systems, more recent focus has shifted toward other applications and functionalities of these structures. The focus of this perspective is on four recent developments in formation and characterization functional, porphyrinic materials and devices: (1) self-assembly and self-organization of porphyrin arrays and aggregates into phototransistors and photonic devices; (2) self-assembled porphyrin squares for sensors, sieves, and catalysts; (3) spatially separated arrays of metalloporphyrins as stochastic sensors; and (4) covalently bound arrays of different chromophores as photonic materials.

KEYWORDS: porphyrins, self-assembly, photonics, catalysts, sensors, arrays

*Correspondence to: Charles Michael Drain, e-mail :cdrain@hunter.cuny.edu

INTRODUCTION

The potential applications of porphyrins in the design of functional materials, sensors, catalysts, and sieves are well documented [1-6]. The rich photo chemistry and redox chemistry is readily modulated by both the natures of the substituents on the macrocycle and of the metallo derivatives. Beyond simple environmental factors that effect any chromophore, further modulation of the chemistry is accomplished by the relative order imposed in supramolecular arrays, crystals, and aggregates formed by self-assembly and self-organization. The nature of the intermolecular interactions (covalent, hydrogen bond, coordination, electrostatic, hydrophobic, etc.) used to form both discrete and polymeric multi-porphyrin systems also helps to dictate the properties, and in the case of structures mediated by coordination chemistry the metal ion linker can add functionality. Stochastic sensors, actuators, and screens using array-based technologies – in the present case using wells of individual metalloporphyrins distributed in arrays on a solid support – is thematically related in that it is the response of the ensemble that provides the enhanced function. This perspective focuses on the recent advances, since 2000, in the applications of porphyrin-based materials from the labs for the four authors.

SELF-ASSEMBLY AND SELF-ORGANIZATION OF PORPHYRIN ARRAYS, AGGREGATES AND DEVICES

Self-assembly and self-organization are widely believed to be central issues to the utilization of nanoscaled materials in real-world fabrication and application of devices based technologies and/or functions exploiting this scale[7]. Conceptually, self-assembly is used to design and form structures wherein the function allows little tolerance for defects and generally uses specific intermolecular interactions to form specific, discrete, supramolecular structures albeit with varying yields. Self-organization, on the other hand, is used when there is more tolerance for defects and generally relies on a combination of non-specific interactions. The inherent redundancies in the latter mitigate the defects, but high quality crystals needed for some applications are a notable exception. In these regards one may look upon the organization and structure of mater into functional nanoscaled materials as falling into four broad motifs. 1. The primary structure is molecular structure – of which we have exquisite control by the highly developed principles of organic chemistry. 2. The secondary structure is supramolecular structure – again a well-developed field based on well-understood principles. 3. The tertiary structure describes how the supermolecules interact to form a higher ordered material that can be aggregate or crystalline – though significant progress has been made to design and predict hierarchical structure, this area is still developing. 4. The quaternary structure describes how the self-assembled and/or self-organized material self-

incorporates into the device or devices and may include the interconnects to the macroscopic world. The quaternary structure is the least developed and the least studied aspect of nanoscaled porphyrinic materials [7].

The tremendous progress in synthetic supramolecular chemistry has yielded a large number of systems wherein two or more porphyrins are self-assembled via a variety of intermolecular forces [1-6]. Both the greater stability and the greater design flexibility afforded by coordination chemistry to self-assemble both discrete and polymeric porphyrinic materials has been exploited to make and characterize a variety of functional materials. On the other hand, the use of complementary hydrogen bonding moieties to stitch together porphyrins has advantages when the self-assembled porphyrin oligomer needs to adapt to its environment in order to self-organize into a functional device. Self-assembled systems using these two specific, directional intermolecular forces can be self-assembled into discrete hierarchical structures via secondary supramolecular synthetic steps, or can self-organize into hierarchical aggregates via non-specific, non-directional interactions such as van der Waals, electrostatic, and hydrophobic. In terms of discrete supramolecular species, both coordination chemistry and hydrogen bonding have been used to make square tetrameric arrays of porphyrins [8-11].

The addition of 12 Pd(II) with labile ligands in the trans position to four 'L'-topic porphyrins which serves as corners, four 'T'-topic porphyrins which serves as the sides, and one '+' topic porphyrin which resides in the center, results in the self-assembly of a planar 3x3 nonamer [12]. The efficiency of self-assembly of these 21 chemical entities is qualitatively the same for both the free base and several metalloporphyrin derivatives. Recent results indicate that the nonamer can be metalated *in situ* by the addition of 9 equivalents of one of several first-row transition metals, which represents the self-assembly of a 30-particle system, Figure 1 [13]! The kinetics of self-assembly the metallononamer and subsequent self-organization of the aggregates are significantly slower, likely because the greatly increased number of possible intermolecular interactions (such as pyridyl coordination to the metal ion, or to a metalloporphyrin), but works because of well understood complexation energetics and kinetics for both the first row metals and palladium. In a second supramolecular synthetic step, a dimer of the 3x3 arrays is nearly quantitatively afforded by the addition of nine equivalents of 4,4'-bipyridine to the all-zinc porphyrin nonamer (before aggregation) to form a sandwich wherein all the porphyrins are in register [12]. Alternatively, the hierarchical self-organization of either the free base or the zinc nonamers into columnar 1-10 nm tall aggregates results in nanoscaled materials with unique properties compared to individual porphyrins, covalent oligomers, large aggregates, or macroscopic materials such as crystals and polymers. The self-organization of nonamers is a secondary process driven largely by pi-stacking and electrostatics. The size of the aggregates is determined by the minimization of particle surface-solvent interactions as is well known for good old-fashioned colloids. The major difference is that each porphyrin in a layer is precisely ordered, while the layers are not ordered with respect to each other. Both of these structural features are important for the photophysical properties of the system, *vide infra* [13, 14].

There are several ways to influence the average length of the columnar aggregates: (1) nature of the R-group decorating the outer edges of the nonamer, (2) metalation state of the porphyrins, (3) nature of the surface the aggregates are deposited on, and (4) it is also possible to trap larger aggregates out of the equilibrating solution. Though this last method traps the kinetic rather than the thermodynamic products, once isolated and dried on a

surface, the structural integrity and photophysical properties of the aggregates are stable for years [13,14]. Both the edge-to-edge interactions in the nonamer, and the face-to-face interactions between layers dictate the properties of the aggregates. Though the heavy atom effect of the Pd(II) quenches the fluorescence of the free base porphyrins by coordination chemistry in the nonamer, and by contact in the aggregates, the aggregates remain luminescent [12]. The addition of 1 to 4 equivalents of a Pd(II) compound with one labile ligand to tetrapyridylporphyrin results in ~67, ~45, ~30, and ~20 % of the observed fluorescence of the un-ligated porphyrin, respectively. This near exponential decrease is what is somewhat higher than expected because of the fact that the heavy atoms are coordinated to the exocyclic pyridyl groups rather than interacting with the porphyrin directly. Additionally, porphyrin fluorescence is well known to be quenched in large aggregates due to a variety of factors such as shading, energy transfer and concomitant branching kinetics, etc. Thus, the luminescence of the nonamer should be much less than the ~ 36% of the collection of un-assembled porphyrins from a statistical estimation of the heavy atom effect. The luminescence is observed; however, to be about 45% of the un-assembled porphyrins and the bands about 10% narrower than expected. These preliminary results indicate that the chromophores in the aggregates are behaving coherently as manifested by the luminescent blinking of individual aggregates. The intensity of the emitted light is constant, but the duration of the 'on' state is not and ranges from less than a second to about a minute! (D. Adams, C.M. Drain, et al, unpublished results)

In another functional mode, metalation of the nonamer with Co(II) (either *in situ* or using the porphyrinato cobalt starting materials) results in a system with nine paramagnetic centers. The self-organization cobalt nonamer into 5-10 nm tall aggregates is somewhat larger than observed for the free base, but can be understood in terms of the increase proclivity for pi-stacking and other electrostatic interactions. As observed in the optical spectra of the parent free base nonamer, in this material the high spin cobalt centers are electronically coupled – albeit weakly – via both the horizontal pyridyl-paladium-pyridyl linkers and the vertical electrostatic interactions. Preliminary magnetic force microscopy results show that the aggregates are indeed magnetic [13,14], but further studies currently underway are required to characterize these properties.

Described below is an example of a functional photo transistor, figure 2, that uses all four levels of self-organization [7, 15]. The synthesis of zinc porphyrin molecules appended with H-bonding or exocyclic ligands represents the primary structure. The self-assembly of these into linear supramolecular arrays is the secondary structure. These self-assembled tapes can be placed in an 8 nm thick by ~1 mm² lipid bilayer separating two compartments with 0.1 M salt solutions where they orient perpendicular to the bilayer-water interface and can adjust their length to the width of the bilayer. The orientation and length adjustment in the bilayer is an example of tertiary organization of matter into a material. The quaternary structure, in terms of a functional device, results when an electron donor (source) is placed on one side of the bilayer, an acceptor on the other side [7,15,16], and calomel electrodes connected to an operational amplifier are placed in the salt solutions on each side of the membrane. In this device white light (or monochromatic light that corresponds to the porphyrin absorption bands) serves as the gate. Thus, when the membrane device is illuminated a photocurrent is observed. The photocurrent depends, of course, on the light intensity, the concentration of self-assembled wires, the dynamics of the membrane, and the diffusion of the donor and acceptor molecules to the bilayer interface. This functional device depends on

nanoscaled supramolecular systems organized into a liquid crystal. It demonstrates that the interconnects to nanoscaled devices need not be nanoscaled *a priori* – as in biology the Grotthus mechanism can be exploited in water, polymers, etc.

APPLICATIONS OF SELF-ASSEMBLED PORPHYRIN SQUARES: CATALYSTS AND SENSORS

Molecular squares are representative of a particular type of self-assembly that has been termed “directed assembly”. Transition-metal based coordination complexes bias or direct the initial stages of the supramolecular synthesis by selectively presenting ligation sites oriented at pre-defined angles with respect to each other [17]. Other factors that can contribute significantly to the efficacy of directed assembly include metal-ligand bond lability [18] and good molecular intermediate solubility [19]. Drain and Lehn have described the directed assembly of a flat porphyrin square featuring L-shaped ligands (5,10-pyridylporphyrin species) and 180°-substituted PtCl₂ linkers [8]. Stang and co-workers have described the formation of an octa-cationic porphyrin square nominally shaped as an open-ended box [20]. This assembly features linear difunctional ligands (5,15-pyridylporphyrins) as walls and uses diphosphine-chelated Pt(II) atoms as 90° connectors at the seams of the box. Slone and Hupp have reported on the assembly of a box-like porphyrin square via reaction of Re(CO)₅Cl with a linear porphyrin ligand (Figure 3) [21]. As shown in the figure’s scheme, the strong trans labilizing effect of CO leads to selective loss of a pair of carbonyls initially ligated cis to each other. This opens up, at each Re center, two coordination sites oriented at ~90° with respect to each other. Progressive coordination of the cis sites with difunctional porphyrin ligands generates a series of right-angle-containing open assemblies that stay in solution because of weak coordination of solvent molecules at remaining sites. Completion of a square and elimination of solvent molecules as ligands is accompanied by precipitation. Among the consequences of this assembly sequence are: 1) high yields, as the equilibrium is pushed toward square formation by removal of the product, and 2) mistake correction via dissociation of undesired open-chain assemblies (soluble assemblies) and re-reaction until closed cycles (squares) are formed.

Multi-metallic porphyrin squares prepared according to Figure 3 have several useful properties. First, despite the presence of Re they display significant photo excited state lifetimes and remain reasonably luminescence [21]. Second, because rhenium is used in oxidation state I (resulting in stable 18-electron organometallic centers) the squares are electrically neutral. This renders them insoluble in aqueous solutions – an important consideration in many thin-film applications. Third, depending on the porphyrin used, the ligand walls define a deep cavity having edge lengths of ca. 18 to 22 angstroms [21,22]. Because the squares lack counter ions, in the solid state the cavities initially contain only solvent molecules. Notably, coordinate-covalent bonds are sufficiently strong (i.e. 4 to 10 times stronger than typical hydrogen bonds) that squares remain intact and cavities persist even after removal of solvent. Fourth, the octahedral coordination geometry of Re(I) offers the possibility of elaboration of the assemblies in the direction normal to the plane of the square – for example, by replacement of chloride ligands with any number of acetylide or di-acetylide terminated moieties.

These properties suggest applications that can capitalize on: a) cavity-containing squares as protective encapsulants for delicate catalysts or as molecular hosts for analytes to be sensed, b) aggregates of squares as

selectively porous molecular materials, and c) isolated squares or ultrathin layers of squares as photochemical sensitizers for redox and energy conversion processes. In our initial studies of supramolecular catalysis, we have observed that encapsulation of an epoxidation catalyst (a manganese-containing di- or tetrapyrrolylporphyrin) by a porphyrin molecular square (**1**) to yield assemblies **2** or **3**, extends the lifetime of the catalyst from about 50 turnovers to more than 20,000 [23]. The observation is reminiscent of the catalyst stabilization achieved with strapped porphyrins and other covalent architectures for active-site protection [24]. A potentially important difference, however, is that the supramolecular assembly is modular: catalysts can be exchanged in and out, and auxiliary sites within the square can be reversibly ligated to alter cavity size, chirality and chemical affinity [23,25]. The functional similarity of the supramolecular catalyst assembly to certain metalloenzymes has been noted: Both types of assemblies employ potent, but indiscriminate catalysts. Selectivity is instead imparted by the surrounding structure – either a tailored square cavity or a protein. In addition, the surroundings serve to prevent catalysts from directly encountering each other and destructively interacting. Extension of the encapsulation idea to arrays of squares comprising substrate-permeable thin films has resulted in enhanced substrate size discrimination and dramatic increases in catalyst lifetime; turnover numbers of greater than 10^6 have been encountered with the limiting factor evidently being the patience of the experimenter rather than the stability of the catalyst.

The existence of well-defined cavities and the comparative ease of preparing low defect films by casting squares from volatile solvents can be exploited for nanoscale sieving. For films prepared on macroporous platforms such as polyester membranes the sieving behavior is easily observed by positioning the membranes as separators in U-cells and monitoring the selective appearance of appropriately sized dye molecules in receiving solutions [26]. Alternatively, by using redox-active probe molecules spanning a wide range of sizes, selective transport can be followed electrochemically [27,28]. These experiments show that size cutoffs can be rationally manipulated by using cavity-functionalized assemblies similar to **2** and **3**. The experiments also show that transport rates vary inversely with molecular film thickness, as expected if film-based diffusion rather than solution-to-film partitioning is the rate-limiting process [27].

For many applications, including separations and catalysis, high molecular fluxes are desirable – something that can be achieved by constructing very thin films. Our experience with molecular films indicates that significant defect-based transport is very difficult to exclude for thicknesses of less than 20 nm. An effective alternative film fabrication strategy uses phenyl-phosphonate functionalized porphyrin squares [29]. By positioning phosphonates at the 10 and 20 positions of the parent porphyrin and square-forming ethynylpyridyl groups at the 5 and 15 positions, we have obtained tetrarhenium squares featuring eight phosphonates – four directed above the plane of the square and four directed below. Advantage can then be taken of the high affinity of phosphonates for Zr(IV) to carry out a layer-by-layer assembly [30] of porous square films; Figure 4. Polarized spectroscopy establishes that films prepared in this way are highly oriented with respect to the surface normal, while AFM measurements of micropatterned films of the parent porphyrin show that film thicknesses can be controlled with extraordinary precision (single molecular layer precision) [31]. Notably, the assembly methodology is sufficiently quantitative that efficient electrochemical sieving can be demonstrated with a single layer. With size exclusion well documented, the obvious next step is to engender selective molecular transport based on chemical properties. In principle, one way of

accomplishing this would be to attach phosphonate-terminated biopolymers or other moieties to the film exterior via Zr(IV). Toward that goal, charge-selective transport has been demonstrated by capping porous porphyrin-phosphonate films with hexaphosphonated coordination complexes having overall 10- charges.

Proof-of-concept studies of porphyrin squares as hosts for molecular or atomic (ionic) guests in chemical sensing studies have focused on two problems: selective recognition of candidate guests and sensitive readout of successful recognition events. The first has been addressed by functionalizing square interiors with appropriate receptors, as shown in Figure 5 [25]. More than 100 cavity variants, including several chiral variants, have been prepared in this way. In illustrative experiments, modest selectivity for alkali metal ions, Zn^{2+} , and molecular iodine as guest species has been observed [32,33]. An alternative approach that is a focus of current work is to gate the entry of guests into extended square channels by appropriately functionalizing channel termini, rather than cavities (channel interiors). This strategy, which can be usefully coupled to related membrane transport and separations problems, has become increasingly attractive as our understanding of how to organize squares as highly oriented thin-film materials has advanced.

The second part of the sensing problem – readout of successful binding by squares – was initially addressed by focusing on the fluorescence of the square and its modulation by guests [32]. The approach proved only partially successful, illustrating the need for a more general readout method. An intriguing alternative has been demonstrated based on micropatterning porphyrin-square films; see Figure 6 [33]. These interesting structures efficiently diffract coherent light – for example, from a laser pointer – to yield a characteristic diffraction pattern. The efficiency of the diffraction process depends on the degree of refractive index contrast between the porous porphyrin film and the surrounding medium (for example, water or air). Uptake of guest molecules increases the average refractive index of the film and increases the diffraction efficiency, a quantity that is easy to evaluate experimentally. The attraction of the method is that it is universal; the only requirement for modulation of index contrast and detection of uptake is that the guest species contain electrons, a condition satisfied by all molecules. A useful variant of the method is one in which the incident light is resonant with an allowed electronic transition of the porous material. Under these conditions, signals can be selectively amplified by as much as three and one half orders of magnitude, greatly improving the sensitivity of the technique while also imparting substantial chemical selectivity at the readout stage [34]. An intriguing extension of the resonance strategy would be to apply it to the multi-chromophoric metalloporphyrin arrays developed by Suslick and co-workers and described further in a following section [35].

Molecular square **1** has a B-band extinction coefficient of about $1.1 \times 10^6 \text{ M}^{-1}\text{cm}^{-1}$, suggesting utility in fundamental energy-transfer studies and in light-harvesting applications. The ability of the square to function as a simple antenna has been noted [21]. Absorbed energy is rapidly transferred to a fifth porphyrin – a dipyritylporphyrin attached to two of the four available Zn(II) sites within the square cavity – where it is re-emitted. Preliminary studies of a related porphyrin square show that it readily sensitizes TiO_2 to visible-light absorption and electricity generation in a Grätzel-type [36] photoelectrochemical cell. The use of porous molecular materials could obviate some significant ion transport problems that plague most multilayer sensitization schemes. In any case, the square is attached to the photoelectrode surface via four of eight available phosphonate groups. The remaining four can be used to bind a second layer of square via the zirconium chemistry described above. Repetition leads to build

up of additional layers and, of course, a systematic increase in film extinction. Curiously, however, additional layers beyond the first two or three layers do not appreciably increase photocurrents. Electronic structure calculations suggest that the effect (or lack of effect) with this first-generation sensitizer is a consequence of orientation of the transition dipole moment for the lowest Q transition in a direction parallel rather than perpendicular to the electrode surface. Thus, efficient lateral energy transfer (column to column EnT) should occur, but at the expense of vertical energy transfer (EnT along the length of a square column). An obvious design objective for second-generation sensitizers is to align transition dipole moments for the lowest energy transitions perpendicular to the surface. Another will be to elaborate on the chromophoric properties so that broader spectral coverage can be obtained.

MULTICHROMOPHORIC SYSTEMS AS COMPONENTS OF PHOTONIC DEVICES

The successful development of new molecule-sized electronics promises to yield dramatic improvements in component density, response speed, and energy efficiency. Given that energy and electron transfer processes within molecules can take place on a sub-picosecond time scale, it is possible in principle to produce devices that function far more rapidly than current devices. We have developed three fundamental approaches to producing molecular switches based on photoinduced electron transfer. One of these strategies modifies the charge transmission characteristics of the bridge molecule in a covalently linked donor-bridge-acceptor system on a picosecond time scale [37]. The second strategy uses photoinduced electron transfer to produce a radical ion pair in the donor-acceptor array: $D^+-A_1^-A_2$. The reduced acceptor A_1^- possesses an intense optical absorption that can be irradiated with a second laser pulse to produce the excited state $D^+-A_1^{*-}A_2$ that is capable of transferring an electron to the secondary acceptor A_2 . We have already demonstrated that sequential application of femtosecond laser pulses to both linear [38] and branched [39,40] systems of this type can propagate the electron up a potential gradient in the linear case, and result in an optically controlled change of electron transport direction in the branched case. The third approach recognizes that the rates of electron transfer reactions can be controlled through the application of electric fields. The electric field produced by a photogenerated ion pair can have a large effect on the electronic states of surrounding molecules. For example, a photogenerated electric field can affect the optical properties of a nearby molecule, or even alter the rate of electron transfer between a second donor-acceptor pair. If each of these processes is photodriven, logical devices can be developed based on the number, sequence, and frequencies of optical pulses used to produce a particular optical observable in these systems.

In the past two years we have developed porphyrin-based molecular systems in which a photogenerated ion pair produces a 10^6 - 10^7 V cm⁻¹ electric field that electrochromically shifts a strong charge transfer optical transition in a neighboring molecule modifying the optical transparency of a sample at a particular set of wavelengths. The overall molecular design of these systems places a molecule that can be influenced by the photogenerated electric field at a fixed distance and orientation relative to the ion pair. In this manner both the magnitude and direction of the electric field are fixed relative to the orientation of the probe molecule. The photogenerated electric field significantly perturbs the electronic structure of a probe molecule having a strong charge transfer transition. This perturbation can be used to carry out switching operations in a repetitive manner on a picosecond time scale.

Molecule **4** has a 9-aminoperylene-3,4-dicarboximide chromophore (C) attached to a zinc 5-phenyl-10,15,20-tripentylporphyrin donor – pyromellitimide acceptor pair (D-A), which undergoes quantitative photoinduced electron transfer to form D^+A^- . Chromophore C exhibits a broad charge transfer band at 535 nm [41]. Selective excitation of C within D-A-C using 530 nm, 130 fs laser pulses produces 1C , which undergoes singlet-singlet energy transfer to produce 1D , which in turn transfers an electron to A. If the D-A-C system is selectively excited with 416 nm, 130 fs laser pulses to produce D^+A^-C prior to excitation of C with 530 nm, 130 fs laser pulses, a 25% lower yield of 1C is generated. The intense local electric field produced by D^+A^- causes a 15 nm electrochromic red shift of the charge transfer absorption of C. Thus, the absorption of C at 530 nm is significantly diminished by the presence of D^+A^- . The need to use two laser pulses with different wavelengths to observe these effects, and the resulting picosecond time response makes it possible to consider applications of this concept in the design of molecular switches.

We are currently exploring modifications to this approach that utilize electric field induced wavelength shifts in fluorescence emission as observables. This should make it possible to produce solid state arrays of these molecules that can be addressed by light pulses with sub-diffraction-limit spatial extent. In this manner it may be possible to produce high-density information processing arrays using this approach. The electrochromic shifts observed in these systems can also be used to develop amplifiers to carry out all optical amplification over a broad range of wavelengths. In these systems the photogenerated electric field effect of D^+A^- is used to gate the transmission of an intense light beam that is normally absorbed by the C chromophore. Ultrafast electrochromic shifting of the absorption band of C results in a large increase in transmission of the second light beam. We are currently exploring amplifier materials over the entire visible wavelength range, as well as optimizing the electronic structures of the chromophores to give large electrochromic wavelength shifts.

A critical step towards photofunctional devices is the ability to create increasingly larger arrays of interactive molecules. Covalent synthesis of large molecular arrays is highly inefficient and costly, thus making self-assembly the method of choice to achieve ordered architectures from functional building blocks. Self-assembly can be based on a variety of weak interactions such as hydrogen bonding and π - π van der Waals interactions as well as covalent bonds. Photosynthesis is an important model for efficient photochemical energy conversion. In contrast to stepwise charge separation in photosynthetic proteins, photoconversion using dye-sensitized semiconductors depends on ultrafast electron injection from the photoexcited dye into the conduction band of the semiconductor followed by rapid charge transport throughout the semiconductor structure.

We have studied a zinc 5,10,15,20-tetrakis(perylene-3,4,9,10-tetracarboxylic diimide) porphyrin, ZnTPP-PDI₄, that self-assembles into ordered photofunctional organic nanoparticles using van der Waals interactions between the individual molecules and exhibits not only the characteristics of an antenna-reaction center complex described above, but demonstrates more extensive charge transport within the nanoparticles as well [42]. The ZnTPP-PDI₄ molecule self-assembles into ordered nanoparticles both in solution and in the solid state driven by van der Waals stacking of the PDI molecules. The optical spectra of the (ZnTPP-PDI₄)_n nanoparticles strongly support the proposed structure depicted schematically in Figure 7.

The PDI molecules most likely stack directly on top of one another in register, presumably at a van der Waals contact distance of about 3.5 Å, while the ZnTPP molecules occupy sites in every other layer with an interlayer Zn-Zn distance of about 7 Å. Photoexcitation of the nanoparticles results in quantitative charge separation in 3.2 ps to form ZnTPP⁺ PDI⁻ radical ion pairs in which the radical anion rapidly migrates to stacked PDI molecules that are on average 5 layers removed from the site of their generation as evidenced by magnetic field effects on the yield of the PDI triplet state that results from radical ion pair recombination. These field effects also show that the electron hopping rate within the PDI stacks is about $2 \times 10^{10} \text{ s}^{-1}$. These nanoparticles exhibit charge transport properties that combine important features from both photosynthetic and semiconductor photoconversion systems.

SENSOR ARRAYS BASED ON METALLOPORPHYRINS

The use of arrays of cross-reactive sensors has become a research area of intense interest over the past decade [43]. Previous sensor arrays have employed a variety of chemical interaction strategies, including the use of conductive polymers [44], conductive polymer/carbon black composites [45], fluorescent dye/polymer systems [46], and polymer coated surface acoustic wave (SAW) devices [47]. In all such sensor arrays, however, the fundamental interaction between the sensor components and the analytes has been weak physical adsorption, which has badly limited the detection sensitivity. Suslick and coworkers [2, 35, 48] have developed a new sensor array technique that makes heavy use of the ligation of analytes to metalloporphyrins in which colorimetric changes in an array of dyes constitute a signal much like that generated by the mammalian olfaction system; each dye is a cross-responsive sensor.

This technology uses a disposable two-dimensional array of chemoresponsive dyes as the primary sensor elements, making it particularly suitable for detecting many of the odiferous compounds produced by bacteria. Striking visual identification of a wide range of volatile organic compounds (VOC's), including carboxylic acids, alcohols, amines, ethers, thioethers, and thiols, are easily made at part per billion (ppb) levels (i.e., sensitivities comparable to or better than gas chromatographic flame ionization (GC-FID) or mass spectrometric (GC-MS) detection).

Design of the Colorimetric Sensor Array

The design of the colorimetric sensor array is based on two fundamental requirements: (1) the chemo-responsive dye must contain a center to interact strongly with analytes, and (2) this interaction center must be strongly coupled to an intense chromophore. The first requirement implies that the interaction must not be simple physical adsorption, but rather must involve bond formation, strong acid-base interactions, or strong dipolar interactions. The consequent dye classes from these requirements are (1) Lewis acid dyes (i.e., metal ion containing dyes), (2) Bronsted acidic or basic dyes (i.e., pH indicators), and (3) dyes with large permanent dipoles (i.e., zwitterionic solvatochromic dyes) (Figure 8).

Metalloporphyrins are a natural choice for the detection of metal-ligating vapors because of their open coordination sites for axial ligation, their large spectral shifts upon ligand binding, and their intense coloration.

Metalloporphyrins have been previously employed for optical detection of gases such as oxygen [49] and ammonia [50], and for vapor detection as chemically interactive layers on quartz crystal microbalances [51].

The large color changes induced in metalloporphyrins upon ligand binding creates a sensitive colorimetric technique that minimizes the need for extensive signal transduction hardware. This represents the first example of a colorimetric array detector for vapor phase ligands and makes it easy to obtain unique color change signatures for analytes for both qualitative recognition and quantitative analysis by simply taking the difference before and after exposure of scanned images of the array

The large spectral changes (and readily observable color changes) that occur in solution during ligand binding to metalloporphyrins have been well documented. Solution studies have indicated that the magnitudes of spectral shifts correlate with the polarizability of the ligand; hence, there exists an electronic basis for analyte distinction. Furthermore, the periphery of the metalloporphyrin can be easily modified, thereby adjusting the accessibility of the metal ion to the ligand and inducing shape-selective ligation. Using metal centers that span a range of chemical hardness and ligand binding affinity and substituents that allow varying access to the metal, a wide range of volatile analytes are differentiable. Porphyrins also show significant solvatochromic effects, so even weakly interacting vapors (e.g., arenes, halocarbons, or ketones) show distinguishable colorimetric effects.

To image the arrays, a glass and Teflon cell holds the array in a fixed position on an inexpensive flatbed scanner while gas containing the analyte(s) of interest flow over the array. The analyte mixture is prepared quantitatively using digital mass flow controllers for serial dilution of commercial permeation tube sources or from saturation towers at carefully thermostated temperatures. Alternatively, a portable hand-held prototype makes use of off-the-shelf inexpensive commercial products: a white LED light source, a micro-air pump, and an ordinary web-camera interfaced to a computer.

With a 6x6 array, as currently finalized, each analyte is represented as a 108-dimensional vector (36 red, green, and blue values) each of which can take on one of 256 possible values (for inexpensive 8 bit digital cameras). The theoretical limit of discrimination, then, would be the number of possible patterns, i.e., $(256)^{108}$. Realistically, however, the RGB vector components do not range over the full 256 possible values; R, G, and B values, however, do vary over a range of 40. To discriminate patterns, let us assume a change of at least 4 is needed in the R, G, or B value (actual discrimination is usually possible with only a change of 2). From principal component analysis, not all of the 108 dimensions are equally important. In fact, roughly 95% of all information is contained in ~15 specific dimensions (i.e., linear combinations of the 108 different R, G, and B values). This implies a 'practical' limit of discrimination that is still immensely large: $(40/4)^{15} = 10^{15}$ distinct patterns should be recognizable in a simple 6x6 array. For a translation of this expectation into chemical terms, the color change profiles of even closely related compounds are distinct. For example, n-butylamine, n-hexylamine, t-butylamine, cyclohexylamine are all differentiable from one another by simple examination of the pattern.

Analysis of Array Responses

No detailed statistical manipulation is necessary to distinguish among the patterns of different analytes, even when they are closely chemically related. The color fingerprint for a given exposure is achieved by simply

differencing the pre- and post-exposure images. This can be accomplished using commercially available software, e.g., Adobe Photoshop, and compared to a library of image data. An example of this differencing is shown in Figure 9.

In order to demonstrate the generality of this sensing technique, a wide range of chemical functionalities have been examined and a comparison of color changes at saturation is shown in Figure 10. Each analyte is easily distinguished from the others, and there are family resemblances among chemically similar species. Analyte distinction originates both in the metal-specific ligation affinities and in their specific, unique color changes upon ligation. Chemometric statistical tools have been used to study the porphyrin array responses. Principal component analysis (PCA) studies revealed that the porphyrin array responses are relatively specific, having a relatively low degree of redundancy. Furthermore, almost all of the chosen metalloporphyrins contribute to analyte distinction, meaning the initial array was well-chosen for the vapor sensing task. Hierarchical cluster analysis (HCA) was used to quantitatively compare vapor fingerprints. The HCA analysis revealed distinction of all of the tested vapors, with groupings formed among similar analytes, such as phosphorus-containing ligands, sulfur-based ligands, and nitrogenous bases. This is unique among electronic nose technologies and means that even in cases where the color change pattern of an unknown analyte is not in the library, one will be able to tell what that analyte most closely resembles in its chemical properties.

The color changes seen in the porphyrin array upon vapor exposure are attributable to ligation of the metal center by the analyte. Diffuse reflectance spectra were obtained for single porphyrin spots both before and after exposure to analyte vapors. Spectral shifts upon analyte exposure correlated well with those seen from solution ligation. For example, Zn(TPP) exposure to ethanol and pyridine vapor gave shifts very similar to those resulting from ligation in methylene chloride solutions containing ethanol and pyridine, respectively.

Further selectivity has recently been incorporated into the array by the use of sterically crowded metalloporphyrins. Sen and Suslick synthesized a new class of bis-pocketed siloxyl-metalloporphyrins in which extreme steric hindrance has been generated on both faces of 5,10,15,20-tetraarylporphyrinatozinc(II) complexes using six, seven, or eight *t*-butyldimethylsiloxyl groups in the ortho-positions [52]. The bulky siloxyl groups were appended to 5-phenyl-10,15,20-tris(2',6'-dihydroxyphenyl)porphyrinatozinc(II) and 5,10,15,20-tetrakis(2',6'-dihydroxyphenyl)porphyrinatozinc(II) to produce highly protected metal sites. These porphyrins display remarkable size and shape-selective ligation of a series of small vaporous organic amines, as shown in Figure 11. All three porphyrins respond to the sterically unencumbered hexylamine, but none respond to the more sterically hindered dipropylamine. The array is even able to differentiate between the very similar pyridine and piperidine; the heptasubstituted TPP shows a greater response for pyridine than for the bulkier piperidine.

Array Sensitivities and Interference

This array detection relies on strong analyte-sensor interactions. Metal-ligand (i.e., metal-analyte) bonds range in their bond enthalpies from ~40 to ~200 kJ/mol. In non-coordinating solvents (e.g., alkanes), equilibrium binding constants are often $>10^6 \text{ M}^{-1}$. For pyridine, the vapor pressure is 0.02 atm at room temperature, so the Raoult's constant is $\sim 2 \times 10^{-3} \text{ atm M}^{-1}$. For a binding constant of $\sim 10^6 \text{ M}^{-1}$, this is equivalent to ~ 2 ppb vapor! In contrast, the

enthalpy of physical adsorption (e.g., into polymers) is only ~5 to 20 kJ/mol (i.e., roughly a tenth of a metal bond). Therefore, the equilibrium constant for adsorption will typically be only about 5×10^{-5} as large as that for ligation to metal ions. Therefore, ligation is intrinsically ~20,000-fold more sensitive than adsorption into polymers. Differences in the sensitivity of detection techniques, of course, can either enhance or diminish this intrinsic advantage of ligation over adsorption.

An example of this extreme sensitivity is shown in Figure 12, which displays the array response to many of the volatile gases commonly released by bacteria.

Changes in humidity are a very serious interference in other electronic nose technology. By using hydrophobic dyes on a hydrophobic substrate, this problem has been eliminated. PVDF membranes of the type used routinely for Western Blots provide excellent good dispersion of the chemoresponsive dyes on the surface, does not interact with the metal atom, and is reflective enough to provide good signal for both scanning and diffuse reflectance spectroscopy. Its hydrophobic nature also prevents interference from water vapor; a color fingerprint generated from exposure of the array to n-hexylamine vapor with 0% relative humidity was identical to that with 100% relative humidity. The insensitivity of this technology gives it a substantial advantage over polymer-based electronic noses, all of which are susceptible to fluctuations in humidity.

OUTLOOK FOR THE FUTURE

The applications and devices described above demonstrate the incredibly diverse potential applications of porphyrins. The stability of the macrocycle is sufficient for many of these to make it into commercially viable applications. Self-assembly greatly reduces the cost of synthesis of multiporphyrin or multichromophoric systems by increasing the yields sometimes by several orders of magnitude compared to the equivalent covalent arrays – if the latter are synthetically accessible at all. However, if crystals are needed the yield of usable materials must be considered. Combinations of chromophores may yield materials with properties unobtainable with single component systems. The application of stochastic methods to analytical chemistry is a burgeoning field, and the multifaceted spectral response of porphyrins and metalloporphyrins to various analytes makes them ideal signal transducers for sensors.

Acknowledgments. JTH gratefully acknowledges the technical and scientific contributions of his co-workers at Northwestern University, as well as the financial support of the National Science Foundation, the U. S. Dept. of Energy Separations and Analysis Program, and the U. S. Dept. of Energy Solar Photochemistry Program for his group's work on sensing + catalysis, sieving, and sensitization, respectively.

REFERENCES

1. Chen C-T and Suslick KS. *Coord. Chem. Rev.* 1993; **128**: 293-322.
2. Chou J-H, Kosal ME, Nalwa HS, Rakow NA and Suslick KS. In *The Porphyrin Handbook*, Vol. 6, Kadish KM, Smith KM, Guillard R. (Eds.) Academic Press: London, 2000; p 43-131.
3. Burrell AK and Wasielewski MR. *J. Porph. & Phthalocyanines* 2000; **4**: 401-406.

4. Burrell AK, Officer DL, Plieger PG and Reid DCW. *Chem. Rev.* 2001; **101**: 2751-2796.
5. Chambron J-C, Heitz V and Sauvage J-P. In *The Porphyrin Handbook*, Vol. 6, Kadish KM, Smith KM, Guillard R. (Eds.) Academic Press: London, 2000; p 1-42.
6. Kobuke Y and Nagata N. *Mol. Cryst. Liq. Cryst.* 2000; **342**: 51-56.
7. Drain CM. *PNAS* 2002; **99**: 5178-5182.
8. Drain CM and Lehn J-M. *J. Chem. Soc., Chem. Commun.* 1994; 2313-2315.
9. Drain CM, Russel KC and Lehn J-M. *Chem. Commun.* 1996; 337-338.
10. Shi X, Barkigia KM, Fajer J and Drain CM. *J. Org. Chem.* 2001; **66**: 6513-6522.
11. Drain CM, Shi X, Milic T and Nifiatis F. *Chem. Commun.* 2001; 287-288.
12. Drain CM, Nifiatis F, Vasenko A and Batteas JD. *Angew. Chem. Int. Ed.* 1998; **37**: 2344-2347.
13. Drain CM, Batteas JD, Flynn GW, Milic T, Chi N, Yablon DG and Sommers H. *PNAS* 2002; **99**: 6498-6502.
14. Milic T, Chi N, Yablon DG, Flynn GW, Batteas JD and Drain CM. *Angew. Chem. Int. Ed.* 2002, **41**: 2117-2119.
15. Drain CM and Mauzerall DC. *Biophysic. Journal* 1992; **63**: 1544-1555
16. Drain CM and Mauzerall D. *Bioelectrochem. Bioenerg.* 1990; **24**: 263-268.
17. Leininger S, Olenyuk B and Stang PJ. *Chem. Rev.* 2000; **100**: 853-907.
18. Davis AV, Yeh RM and Raymond KN. *PNAS* 2002; **99**: 4793-4796.
19. Slone RV, Benkstein KD, Bélanger S, Hupp JT, Guzei IA and Rheingold AL. *Coord. Chem. Rev.* 1998; **171**: 221-243.
20. Stang PJ, Fan J and Olenyuk B. *Chem Commun.* 1997; **15**: 1453-1454.
21. Slone RA and Hupp JT. *Inorg. Chem.* 1997; **36**: 5422-5423.
22. Zhang J, Williams ME, Keefe MH, Morris GA, Nguyen ST and Hupp JT. *Electrochem. Solid State Lett.* 2002; **5**: E25-E28.
23. Merlau ML, del Pilar Mejia M, Nguyen ST and Hupp JT. *Angew. Chem. Int. Ed.* 2001; **40**: 4369-4372.
24. Collman, JP, Lee VJ, Kellenyuen CJ, Zhang XM, Ibers JA and Brauman JI. *J. Am. Chem. Soc.* 1995; **117**: 692-703.
25. Bélanger S, Keefe MH, Welch J and Hupp JT. *Coord. Chem. Rev.* 1999; **192**: 29-45.
26. Czaplewski KF, Snurr RQ and Hupp JT. *Adv. Mater.* 2001; **13**: 1895-1897.
27. Williams ME and Hupp JT. *J. Phys Chem. B* 2001; **105**: 8944-8950.
28. Bélanger S and Hupp JT. *Angew. Chem. Int. Ed.* 1999; **38**: 2222-2224.
29. Wightman MD. M.S. Thesis, Dept. of Chemistry, Northwestern University, 2001.
30. Coa G, Hong H-G and Mallouk TE. *Acc. Chem. Res.*, 1992; **25**: 420-427.
31. Massari AM, Wightman MD, Gurney RW, Huang C-HK, Nguyen ST and Hupp JT. *Polyhedron* 2002; submitted.
32. Chang SH, Chung K-B, Slone RV and Hupp JT. *Synth. Metals* 2001; **117**: 215-217.
33. Mines GA, Tzeng B, Stevenson KJ, Li J and Hupp JT. *Angew. Chem.* 2002; **41**: 154-157.
34. Bailey RC and Hupp JT. *J. Am. Chem. Soc.* 2002; in press.

35. Rakow NA and Suslick KS. *Nature (London, U.K.)* 2000; **406**: 710-713.
36. Hagfeldt A and Gratzel M. *Acc. Chem. Res.* 2000; **33**: 269-277.
37. Hayes RT, Wasielewski MR and Gosztola D. *J. Am. Chem. Soc.* 2000; **122**: 5563-5567.
38. Debreczeny MP, Svec WA, Marsh EM and Wasielewski MR. *J. Am. Chem. Soc.* 1996; **118**: 8174-8175.
39. Lukas AS and Wasielewski MR. *J. Phys. Chem. B* 2000; **104**: 931-940.
40. Lukas AS, Bushard PJ and Wasielewski MR. *J. Am. Chem. Soc.* 2001; **123**: 2440-2441.
41. Miller SE, Zhao Y, Schaller R, Mulloni V, Just EM, Johnson RC and Wasielewski MR. *Chem. Phys.* 2002; **275**: 167-183.
42. van der Boom T, Hayes RT, Zhao Y, Bushard P J, Weiss EA and Wasielewski MR. *J. Am. Chem. Soc.* (in press).
43. Stetter JR and Pensrose WR. (Eds.) *Artificial Chemical Sensing: Olfaction and the Electronic Nose* Electrochem. Soc.: Pennington, NJ, 2001.
44. Freund MS and Lewis NS. *Proc. Natl. Acad. Sci. USA* 1995; **92**: 2652-2656.
45. Lonergan MC, Severin EJ, Doleman BJ, Beaber SA, Grubbs, RH and Lewis NS. *Chem. Mater.* 1996; **8**: 2298-2312.
46. Walt DR. *Acc. Chem. Res.* 1998; **31**: 267-278.
47. Grate JW, Martin SJ, and White RM. *Anal. Chem.* 1993; **65**: 940A.
48. Suslick KS and Rakow NA. In *Artificial Chemical Sensing: Olfaction and the Electronic Nose*, Stetter JR, Pensrose WR. (Eds.) Electrochem. Soc.: Pennington, NJ, 2001; p 8-14.
49. Baron AE, Danielson JDS, Gouterman M, Wan JR and Callis JB. *Rev. Sci. Instrum.* 1993; **64**: 3394-3402.
50. Vaughan AA, Baron MG and Narayanaswamy R. *Analytical Communications* 1996; **33**: 393-396.
51. Andersson M, Holmberg M, Lundstrom I, Lloyd-Spetz A, Martensson P, Paolesse R, Falconi C, Proietti E, Di Natale C and D'Amico A. *Sensors & Actuators B-Chemical* 2001; **77**: 567-571.
52. Sen A and Suslick KS. *J. Am. Chem. Soc.* 2000; **122**: 11565-11566.

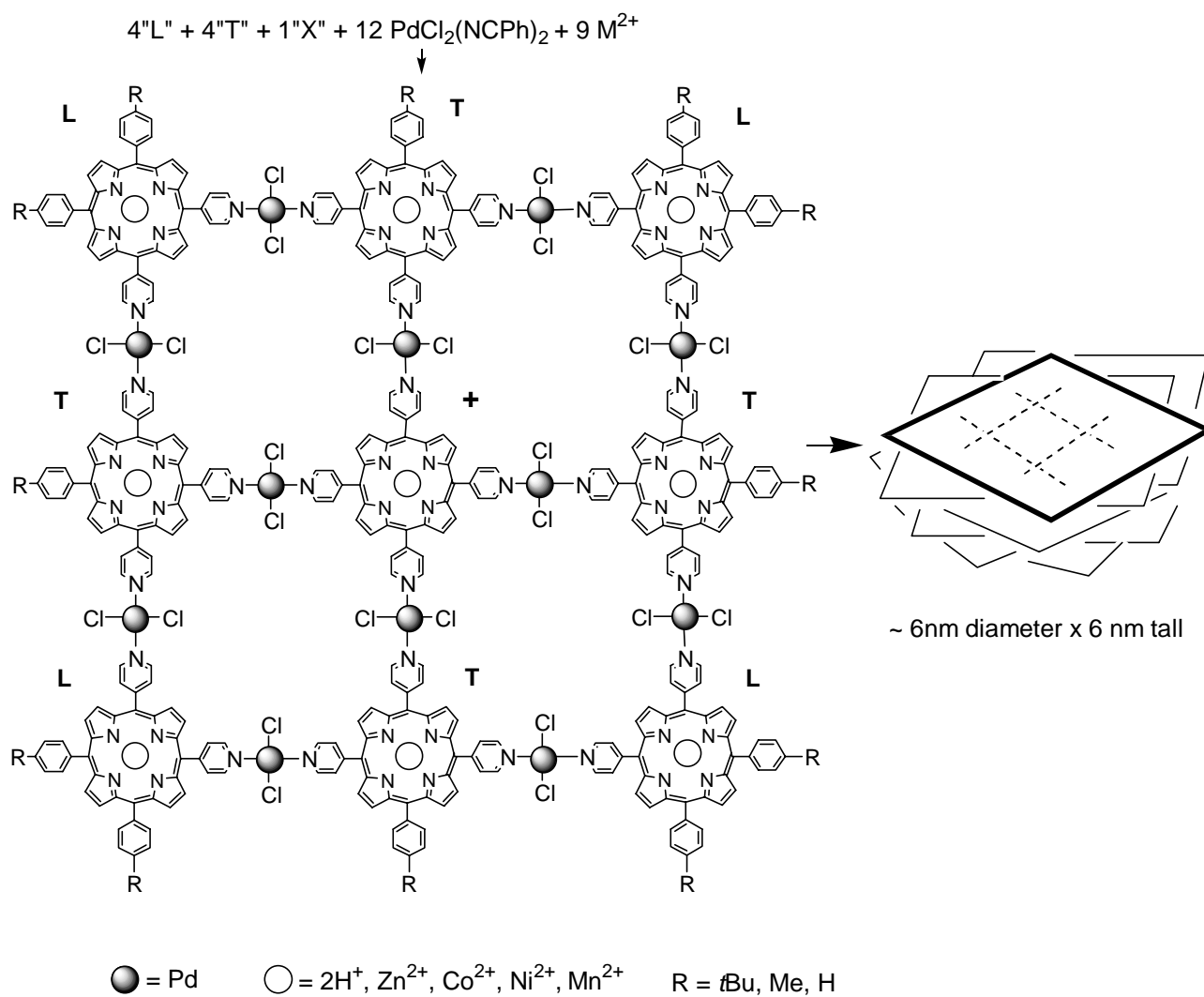


Fig. 1.

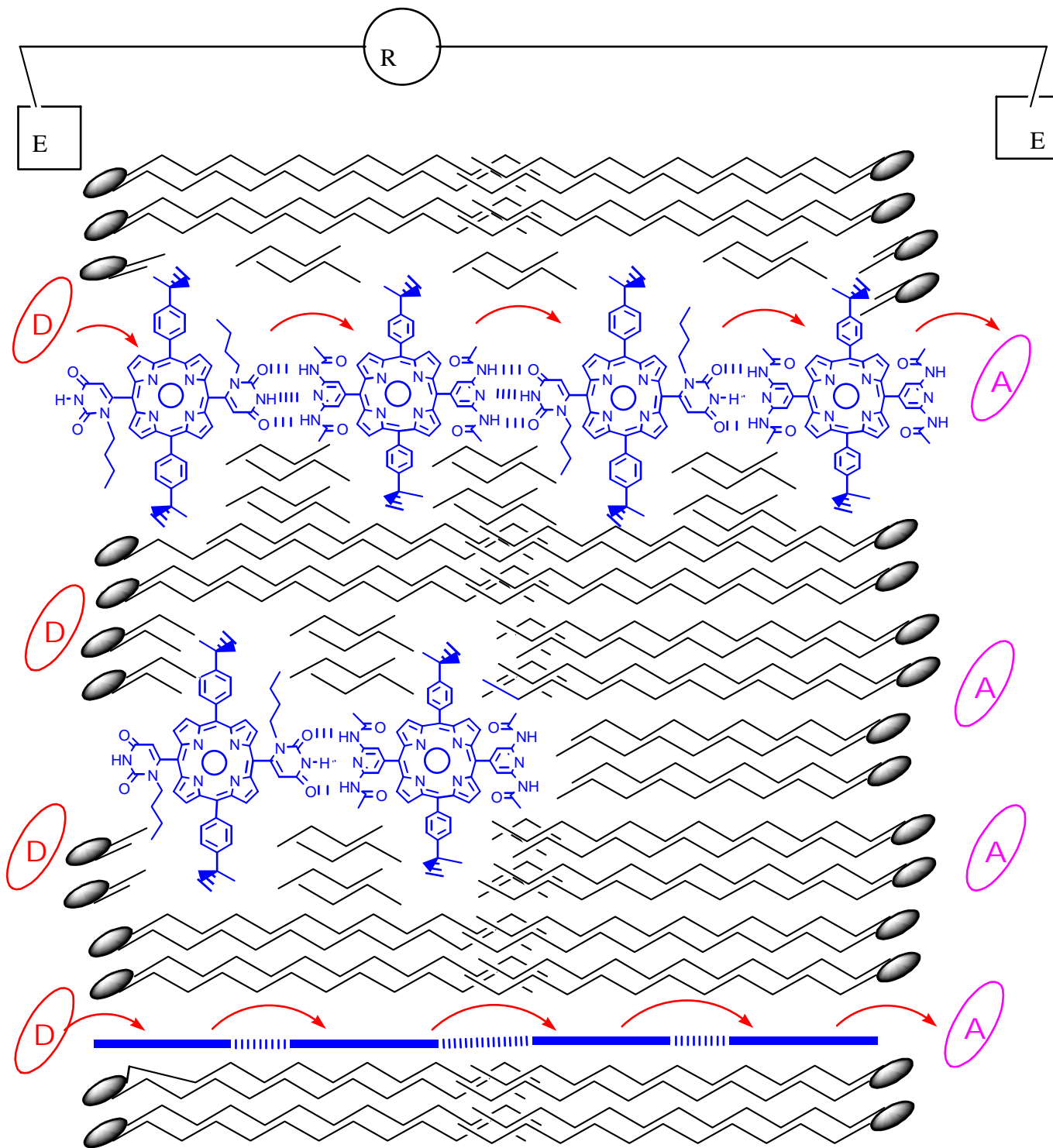


Fig. 2a.

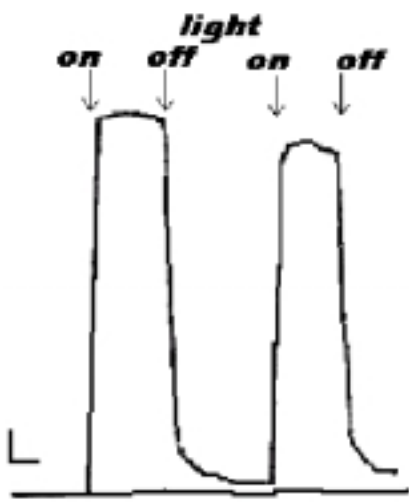


Fig. 2b.

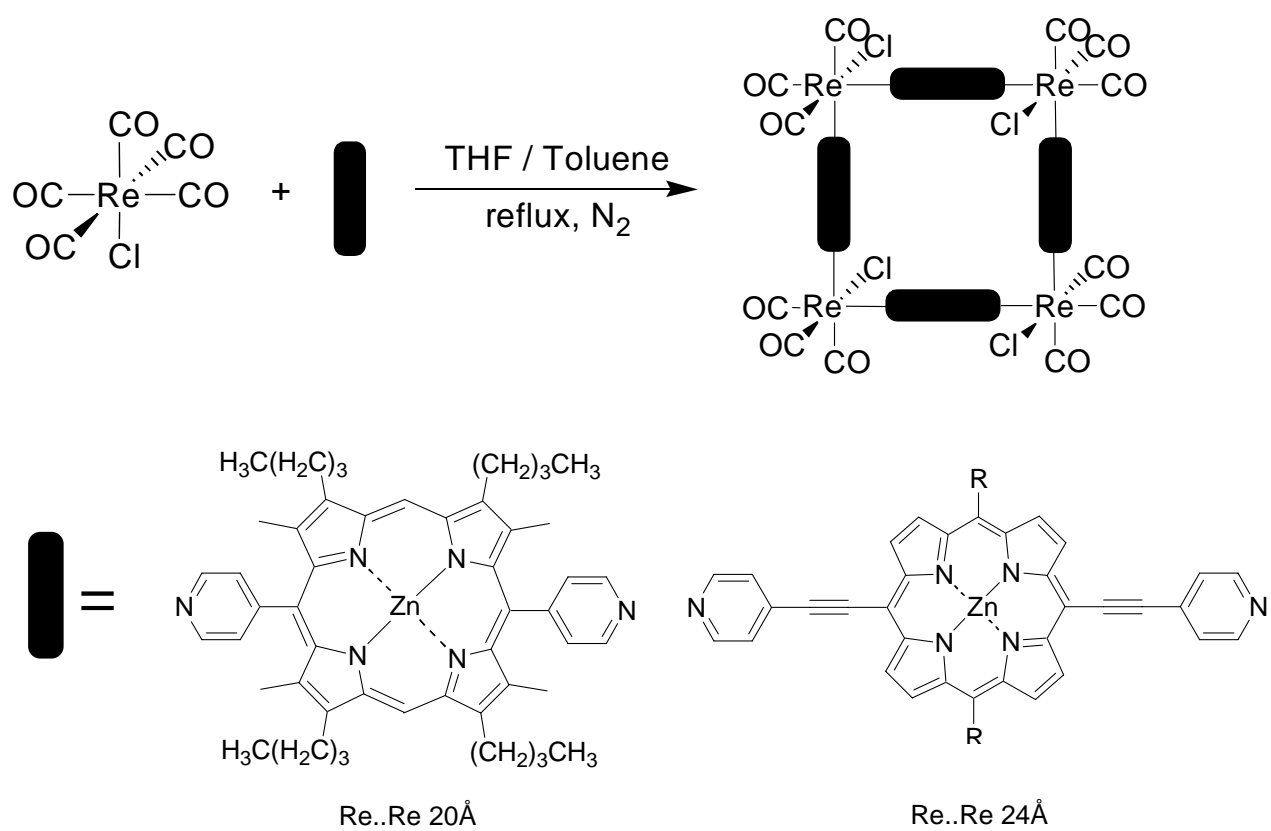


Fig. 3. Directed assembly of porphyrin squares from dipyriddy edge ligands and $\text{Re}(\text{CO})_5\text{Cl}$. The smaller square corresponds to assembly 1.

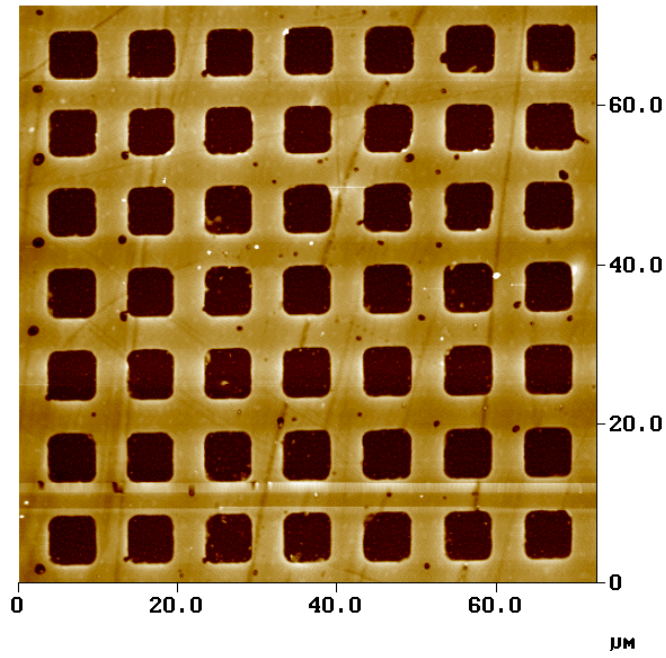


Fig. 4. Low-resolution atomic force microscopy image of a micropatterned film square **1**. The pattern periodicity is 10 microns and the pattern height is ca. 200 to 250 nm.

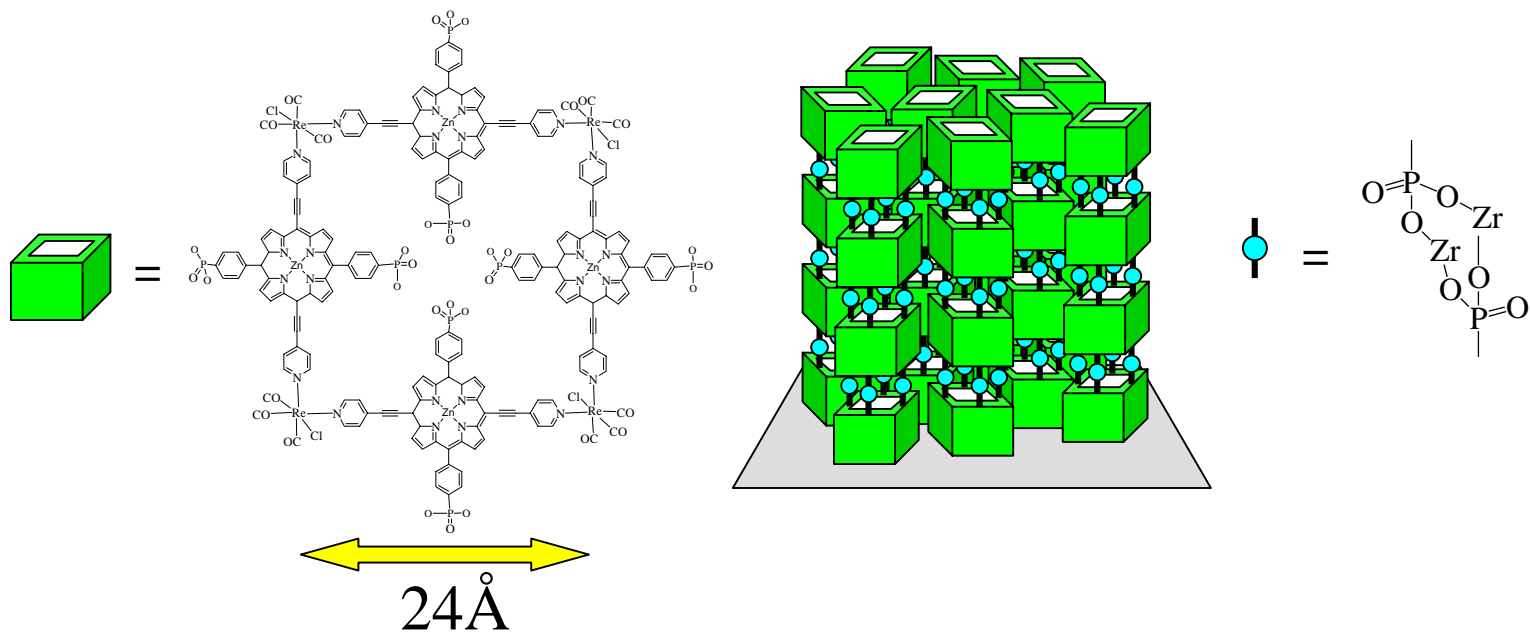
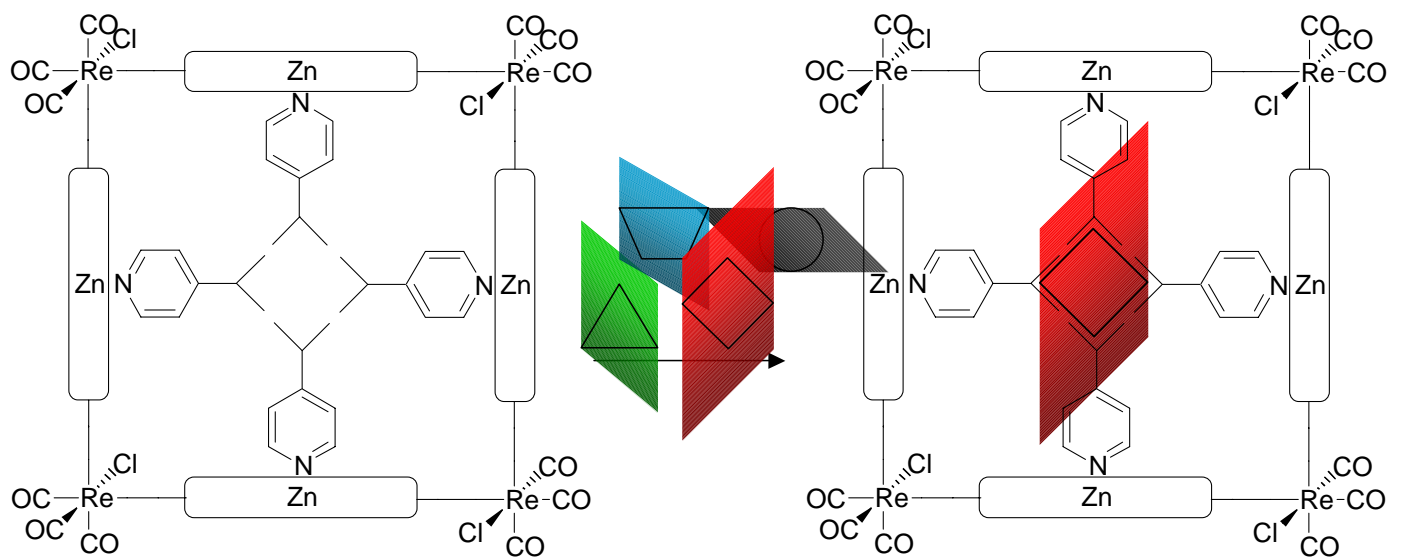
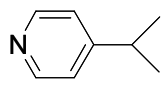
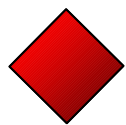


Fig. 5. Layer-by-layer porphyrin square film assembly scheme.



 = Tunable unit which alters binding pocket properties

 = Secondary guest within modified cavity

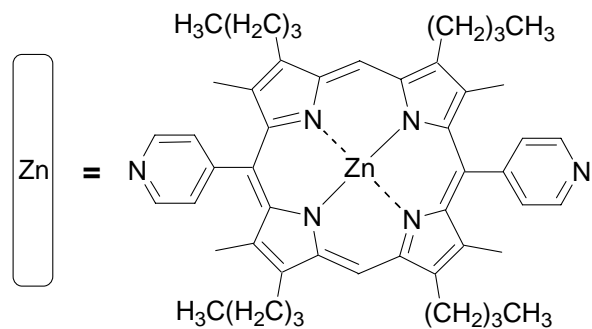
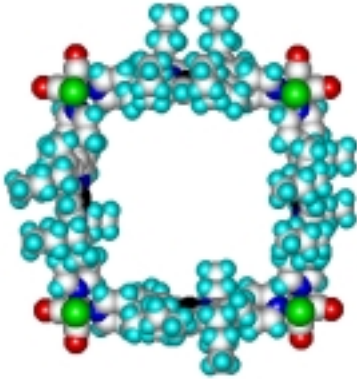
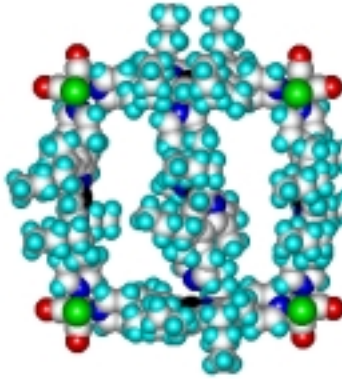


Fig. 6. Schematic representation of cavity functionalization scheme and application of the functionalized cavity selective guest recognition.

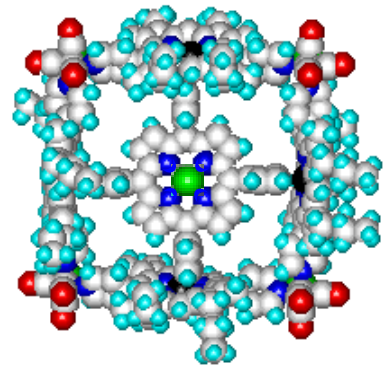
(structures)



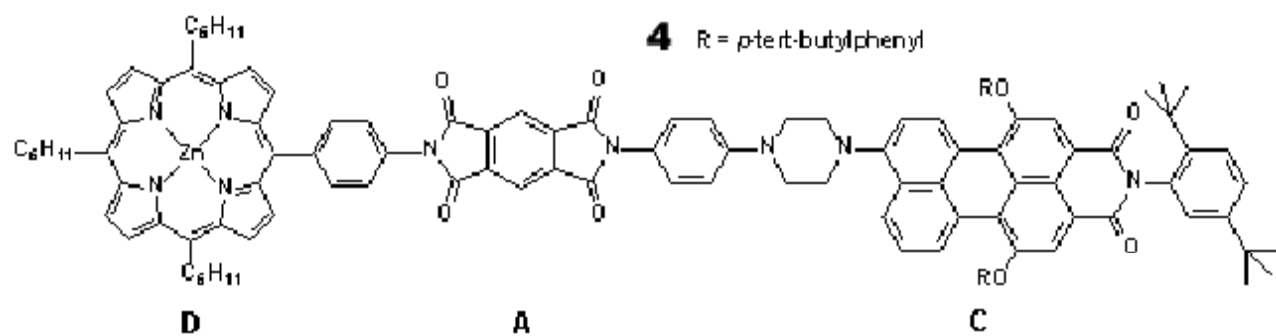
1

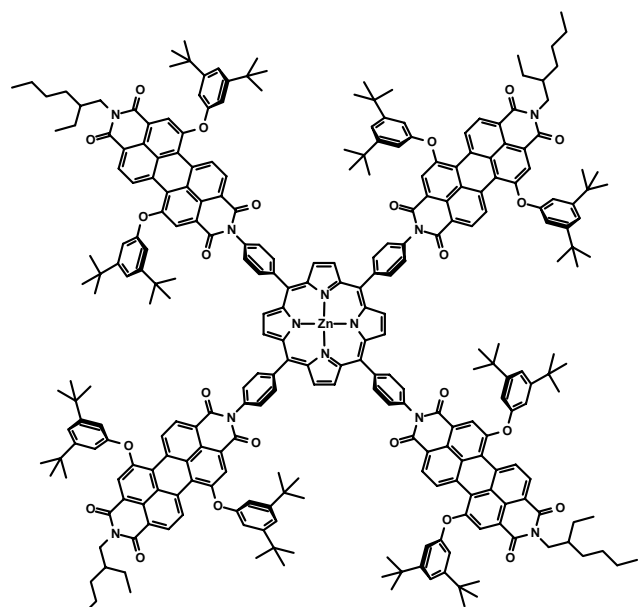


2



3





ZnTPP-PDI₄

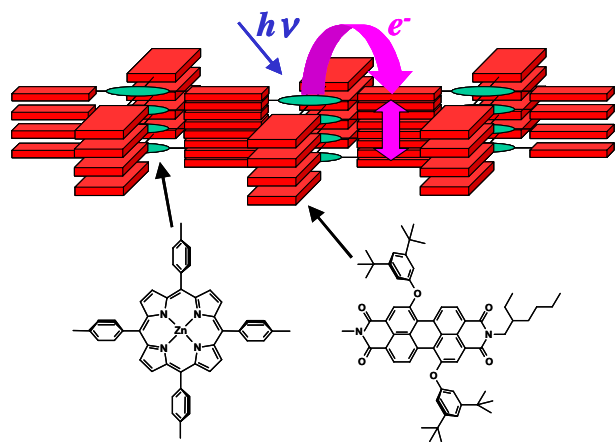


Fig. 7.

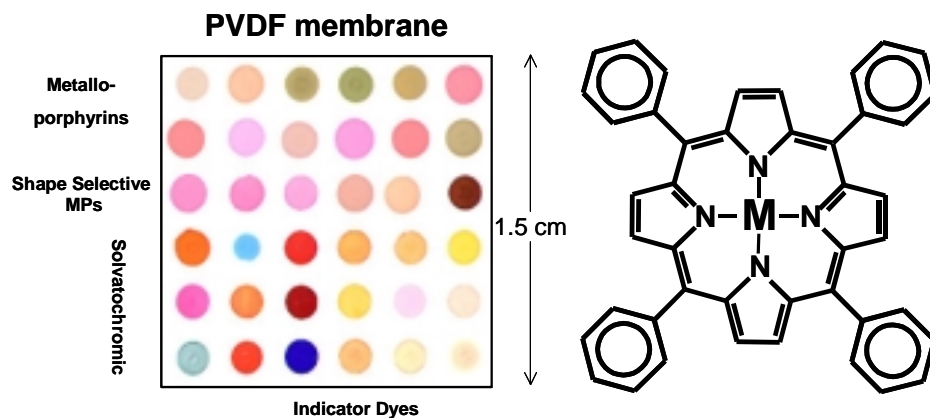


Fig. 8. The colorimetric cross-reactive vapor sensor array. The chemical structure of metalated 5,10,15,20-tetraphenylporphyrins, MTPP is shown. TPP^{2-} is a dianion capable of strongly binding most M(II) and M(III) metal ions.

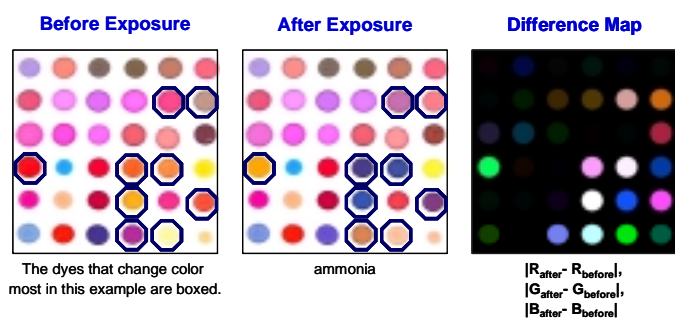


Fig. 9. Difference map of the chemoresponsive dye array provides a color “fingerprint” for any analyte or mixture of analytes.

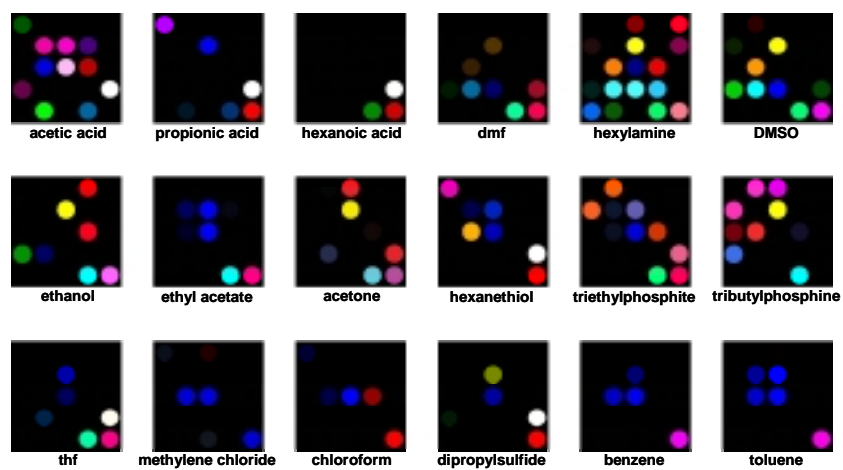


Fig. 10. Color fingerprints for a variety of analytes at saturation vapor pressure. These images result from differencing the images collected before and after exposure to analyte vapor. (These images, of course, are much more dramatic in color than in gray scale.)

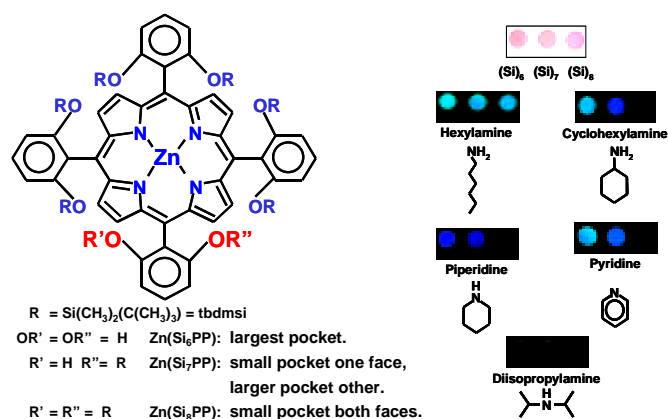


Fig. 11. Left: Structure of shape-selective siloxylporphyrins. Right: Colorimetric response of shape selective siloxylporphyrins to several electronically similar, but sterically different analytes. The rest of the array distinguishes among 1°, 2°, 3°, and aromatic amines.

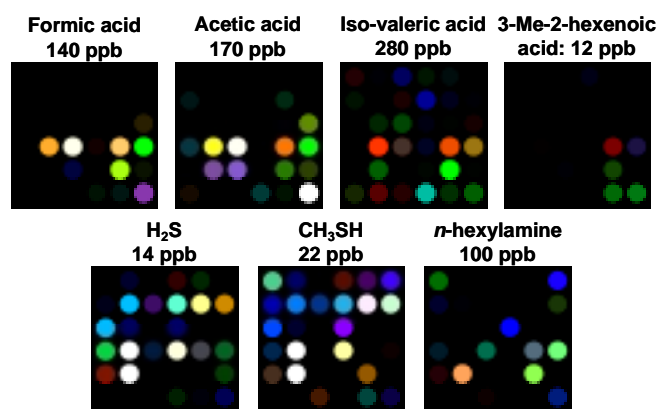


Fig. 12. Part per billion responses to volatile vapors produced by bacterial growth.